Published in final edited form as:
Biochim Biophys Acta. 2014 September ; 1838(9): 2296–2305. doi:10.1016/j.bbamem.2014.02.005.

Branched amphiphilic peptide capsules: Cellular uptake and retention of encapsulated solutes☆

Pinakin Sukthankar[a], **L. Adriana Avila**[a], **Susan K. Whitaker**[a], **Takeo Iwamoto**[b], **Alfred Morgenstern**[c], **Christos Apostolidis**[c], **Ke Liu**[d], **Robert P. Hanzlik**[d], **Ekaterina Dadachova**[e], and **John M. Tomich**[a,*]

[a]Department of Biochemistry and Molecular Biophysics, Kansas State University, Manhattan, KS 66502, USA

[b]Division of Biochemistry, Core Research Facilities, Jikei University School of Medicine, Tokyo 105-8461, Japan

[c]European Commission, Joint Research Centre, Institute for Transuranium Elements, P.O. Box 2340, D-76125 Karlsruhe, Germany

[d]Department of Medicinal Chemistry, University of Kansas, Lawrence, KS 66045-7582, USA

[e]Department of Radiology, Albert Einstein College of Medicine, 1695A Eastchester Rd., Bronx, NY 10461, USA

Abstract

Branched amphiphilic peptide capsules (BAPCs) are peptide nanospheres comprised of equimolar proportions of two branched peptide sequences bis(FLIVI)-K-KKKK and bis(FLIVIGSII)-K-KKKK that self-assemble to form bi-layer delimited capsules. In two recent publications we described the lipid analogous characteristics of our BAPCs, examined their initial assembly, mode of fusion, solute encapsulation, and resizing and delineated their capability to be maintained at a specific size by storing them at 4 °C. In this report we describe the stability, size limitations of encapsulation, cellular localization, retention and, bio-distribution of the BAPCs in vivo. The ability of our constructs to retain alpha particle emitting radionuclides without any apparent leakage and their persistence in the peri-nuclear region of the cell for extended periods of time, coupled with their ease of preparation and potential tune-ability, makes them attractive as biocompatible carriers for targeted cancer therapy using particle emitting radioisotopes. This article is part of a Special Issue entitled: Interfacially active peptides and proteins.

☆This article is part of a Special Issue entitled: Interfacially active peptides and proteins.

*Corresponding author. jtomich@ksu.edu (J.M. Tomich).

Author contributions

The manuscript was written through contributions of all authors. All authors have given approval to the final version of the manuscript.

Keywords

Peptide capsule; BAPC; Self-assembling peptide; Nanocapsule; ^{225}Actinium; Alpha particle therapy

1. Introduction

There is a great deal of interest in the area of nanoparticle-mediated therapies. Nanocarrier mediated targeted cellular therapy is a rapidly growing area of research for the treatment of malignant and infectious diseases. Particle emitting radioisotopes complemented with a targeting moiety are being recognized as some of the most promising cytotoxic candidates for the treatment of cancerous tumors. Nano-particles enjoy distinct advantages in the delivery of drug payloads. Their nanosizes enable them to be directly injected into systemic circulation [1,2] and afford them longer circulating times [3,4]. Furthermore, the circulating time can be increased by the surface modification of nano-particles with hydrophilic moieties such as polyethylene glycol [5–7], and nanoparticles composed of biodegradable polymers can be tuned to release their drug payload in a controlled fashion; either by micelle dissociation, polymer degradation, diffusion or in combination [8–10]. Mechanisms of nanoparticle internalization into cells are influenced by their physiochemical properties. Biocompatible nanocomposites such as lipid based carriers (liposomes and micelles); polymeric vesicles designed from amphiphilic block co-polymers [11] such as polyethylene glycol–polylactic acid (PEG–PLA) and PEG–polycaprolactone (PEG–PCL) [12]; nanocapsules [13,14], bola-amphiphiles (amphiphilic molecules possessing two polar heads on both sides of an aliphatic chain) such as aminoundecyltriethoxysilane (AUT) [15,16]; and carbon nanotubes [17] have been studied for their efficacy as delivery systems.

Liposomes are preferred over other delivery systems due to their ability to encapsulate both hydrophobic and hydrophilic contents. They can also be modified with respect to their fatty acid and head group composition, and surface alterations to modulate drug release and target affinity. Some of the issues associated with liposomes such as degradation by hydrolysis, oxidation, sedimentation, aggregation, or fusion during storage are being addressed with the development of niosomes [18] and proniosomes [19,20], however further testing is needed to fully establish safety and efficacy.

The selection of any nanoparticle for a specific pharmacological use is contingent on its mechanism of cellular uptake and intracellular trafficking [21]. In addition, concerns relating to the successful encapsulation of cargo, stability, specificity, bio-reactivity, biodegradability and toxicity are also relevant. The ability to release their contents is not necessarily a requirement for certain cargos. In the case of targeted alpha particle therapy (TAT) – a treatment modality for metastatic cancer and infectious diseases – the advantageous properties of ^{225}Ac [22] are partially offset by its systemic toxicity [23] due to the potential accumulation of its daughter nuclides in off-target sites. Utilization of alpha-emitters requires containment systems that allow the high-energy alpha particles to penetrate target tissues while retaining the radionuclide and its daughter isotopes. This poses a considerable challenge since the energy (5 to 8 MeV/^{225}Ac α-particle) released is sufficient to disrupt the integrity of most traditional nano-carriers. This property has hampered the

development of ^{225}Ac as a viable radio-therapeutic agent [24,25]. The current use of chelating agents for ^{225}Ac radioimmunotherapy has been challenging as a consequence of the poorly defined coordination chemistry of Ac(III), owing to the lack of stable isotopes to enable routine chemical analysis [26]. Chelators like EDTA, DTPA, DOTA and PEPA [27,28] have been used to complex with ^{225}Ac with varying degrees of success. On the other hand the potential of the otherwise promising ^{225}Ac-HEHA macrocyclic complex in radiotherapy [29] has been marred by instability, due to the coordinated ^{225}Ac radionuclide decaying into its daughter isotopes [26].

Efforts to develop bifunctional chelators capable of stably binding ^{225}Ac to antibodies as well as competently containing resulting daughter nuclides at target sites, have not been successful. This has forced the development of sterically stabilized pegylated liposomes [30] and stable pegylated phosphatidylcholine–cholesterol liposomes [31] for radioimmunotherapeutic applications despite the inherent instability and retention based limitations associated with traditional liposomal systems. Moreover, novel liposomal carriers such as MUVELs (Multivesicular liposomes) – involving the passive entrapment of small vesicles into large liposomes – have been designed to enhance the targeting capabilities and the retention of alpha particle emitting daughters of ^{225}Ac, in an effort to better utilize their positive cytotoxic potential [32]. All of this liposome directed encapsulation techniques are however lengthy and tedious; [30–32] and involve considerable preparation times that include complex formation of ^{225}Ac with a chelate, annealing procedures, extended waiting periods, extrusions and centrifugation; apart from addressing various issues to counter physiochemical problems such as possible oxidation due to alpha emissions [33,34] and beta [35] and gamma [36] radiation. The work presented herein presents an alternative and flexible means of radionuclide encapsulation that is easy to perform and generates stable in vivo constructs.

Peptide based nano-assemblies show promise as nano-delivery vehicles for the safe, targeted transport of drugs to specific tissues and organs, with minimal off target accumulation [37] by overcoming some of the problems associated with traditional lipid and viral based delivery systems. BAPCs (Branched Amphiphilic Peptide Capsules) are a new class of self-assembling peptide nano-capsular spheres [38,39] formed during the cooperative association of a mixture of two (15–23 residue) poly-cationic branched amphiphilic peptides (Fig. 1). The hydrophobic core sequences are derived from an internal fragment of CaIVS3, the human dihydropyridine sensitive L-type calcium channel segment [40]. The ability of the BAPCs to form bilayer-delimited spheres (Fig. 2) capable of trapping solutes is a consequence of the unique characteristics of its constituent peptides — bis(FLIVI)-K-K_4 and bis(FLIVIGSII)-K-K_4, which reversibly transition from an alpha helical conformation in 2,2,2-Trifluoroethanol, to a beta sheet in water [38,39]. The branch point lysine in the sequence orients the two peptide segments at ~90° angle, mimicking the geometry of diacyl phospholipids. Coarse grain molecular dynamic simulations, [38] consistent with S/TEM analysis, indicate the presence of a single capsular bilayer (3–4 nm) comparable to that of a phospholipid system, which is below the discerning resolution of electron microscopy.

Recently, we described how the flexible BAPCs possess many of the properties of phospholipid vesicles, such as fusion, solute encapsulation and an ability to be resized by

membrane extrusion through polycar-bonate filters with defined pore sizes [39]. We also demonstrated several biophysical characteristics including, their mode of assembly, high thermodynamic stability, and their kinetics of fusion. The BAPCs can –like their lipid counterparts – be both resized, and maintained there by placing them at 4 °C. The versatility of these peptides to self-assemble enables us to tag individual monomers with ligands and molecular markers for a variety of analytical and functional assays, making these constructs particularly suited as biocompatible vehicles for the targeted delivery of cargo into the cells. In this report, we study the stability, cellular uptake, load capacity, retention within biological environments for extended periods of time, tolerance to a radionuclide load, biodistribution and capacity to maintain their structural integrity even when subjected to alpha particle emissions.

2. Materials and methods

2.1. Peptide synthesis

2.1.1. Synthesis of bis(FLIVI)-K-K_4 and bis(FLIVIGSII)-K-K_4 variants—Peptides were synthesized using solid phase peptide chemistry on 4-(2,4-dimethoxyphenyl-Fmoc-aminomethyl) phenoxyacetyl-norleucyl-cross-linked ethoxylate acrylate resin [41] (Peptides International Inc.; Louisville, Kentucky) on a 0.1 mmol scale using Fmoc (N-(9-fluorenyl) methoxycarbonyl)/tert-butyl chemistry on an ABI Model 431 peptide synthesizer (Applied Biosystems; Foster City, CA). This resin yields the carboxyamide at the C-terminus upon cleavage. The Fmoc amino acids were obtained from Anaspec, Inc. (Fremont, CA). The branch point was introduced by incorporating $N^{\alpha,\varepsilon}$ di-Fmoc-L-lysine in the fifth position from the C-terminus. Deprotection of the two Fmoc protecting groups leads to the generation of two reactive sites that allow for the generation of the bifurcated peptide branch point. This enables the simultaneous addition of either of the hydrophobic tail segments, FLIVI and FLIVIGSII to the common hydrophilic oligo-lysine segment by the stepwise addition of Fmoc amino acids [42]. The N-termini of the peptide were acetylated on the resin using Acetic Anhydride/N, N-Diisopropylethylamine/1-Hydroxybenzotriazole prior to cleavage. The peptide was cleaved from the resin using Trifluoroacetic acid (TFA)/H_2O (98:2, v/v) for 90 min at RT. The released peptide product was washed 3× with diethyl ether and re-dissolved in water prior to lyophilization. The water used throughout this study is deionized, reverse osmosis treated and then distilled. The RP-HPLC purified peptides were dried in vacuo and characterized on a Bruker Ultraex III matrix-assisted laser desorption ionization time of flight mass spectrometer (MALDI TOF/TOF) (Bruker Daltonics, Billerica, MA) using 2,5-dihydroxybenzoic acid matrix (Sigma-Aldrich Corp., St. Louis, MO). The dried peptides were stored at RT.

2.1.2. Synthesis of Rhodamine labeled peptide bis(FLIVI)-K-K_4—‘Dye labeled peptides’ were synthesized by solid phase peptide chemistry on a 0.1 mmol scale on MBHA [43] (4-methylbenzhydrylamine) resin (Anaspec, Inc., Fremont, CA). After coupling the first amino acid (N^{α}-Fmoc-N^{ε}-*t*-Boc-L-lysine), the resin was treated with TFA/ Dichloromethane/H_2O (80:18:2, v/v/v) for 30 min to remove the side chain *t*-butoxycarbonyl protecting group; exposing the lysyl ε amine. This was then manually reacted with the N-Hydroxysuccinimide ester of Rhodamine B (Sigma-Aldrich Corp., St.

Louis, MO) in presence of N-N-Diisopropylethylamine to generate the label on the C-terminal lysine. The N^{α}-Fmoc was de-protected and the remainder of the synthesis was carried out as indicated earlier. The labeled peptide was cleaved from the resin using standard HF cleavage protocol [44,45]. The concentrations of all peptides were calculated using the molar extinction coefficient (ε) of phenylalanine residues (two per sequence) at 257.5 nm (195 cm^{-1} M^{-1}) [46,47] on a CARY 50 Bio UV/Vis spectrophotometer (Varian Inc., Palo Alto, CA) using a 0.3 cm path length quartz cuvette (Starna Cells Inc., Atascadero, CA). The Rhodamine B adducted sequences were incorporated at a prescribed mole percentage along with the unlabeled bis(FLIVI)-K-K_4 sequence of the BAPCs and utilized in fluorescence experiments.

2.1.3. Synthesis of Pep-1—Pep-1 (Ac-KETWWETWWTEWSQPKKKRKV-CONH-$(CH_2)_2$-SH) was synthesized by solid phase peptide synthesis using Fmoc-Cysteamine-SASRIN™ resin, 0.6 meq/g, (Bachem, Torrance, CA) on an Applied Biosystems 431A Peptide Synthesizer at a 0.1 mmol scale using standard Fmoc(N-(9-Fluorenyl)methoxycarbonyl)/tert-butyl chemistry as described [42]. The Fmoc amino acids used for the synthesis were obtained from Anaspec, Inc. (Fremont, CA). The N-terminal amino group was acetylated and the peptide was cleaved from the resin using TFA/water/triisopropylsilane (94:4:2, v/v/v) for 90 min at RT to generate the C-terminal thiol. The peptide product was washed 3× with diethylether and redissolved in water prior to lyophilization. This was then purified using Reversed Phase-HPLC with 0.1% TFA/H_2O and 0.1%TFA/90% Acetonitrile, as the binary solvent system. The purified peptide was dried in vacuo and characterized on a Bruker Ultraflex III matrix-assisted laser desorption ionization time of fiight mass spectrometer (MALDI TOF/TOF) (Bruker Daltonics, Billerica, MA) using α-Cyano-4-hydroxycinnamic acid matrix (Sigma-Aldrich Corp., St. Louis, MO). The dried peptides were stored at RT.

2.2. Capsule formation and encapsulation

The bis(FLIVI)-K-KKKK and bis(FLIVIGSII)-K-KKKK peptides were dissolved individually in neat 2,2,2-Trifluoroethanol (TFE, Sigma-Aldrich Corp, St. Louis, MO). In this solvent the peptides are helical and monomeric thereby ensuring complete mixing when combined. Concentrations were determined as diluted samples in water using the absorbance of phenylalanine as described in Section 2.1.2. The bis(FLIVI)-K-KKKK and bis(FLIVIGSII)-K-KKKK peptide samples were mixed in equimolar ratios to generate a fixed calculated concentration of 0.1 mM in the final volume(s), then dried in vacuo. The dried peptide samples were then hydrated to form capsules of desired concentration by the drop-wise addition of water.

2.3. HeLa cell culture

HeLa cells were obtained from Dr. Stella Y. Lee's laboratory (Division of Biology, Kansas State University) and grown in Dulbecco's minimum essential medium (Life Technologies, Grand Island, NY) with 10% fetal bovine serum. Cell cultures were passaged every 3rd–4th day by trypsinizing them using TrypLETM Express (Life Technologies, Grand Island, NY) and were kept in a humidified incubator at 37 °C and 5% CO_2. The media were replaced every 72 h with no addition of antibiotics.

2.4. Cellular uptake of branched amphiphilic peptide capsules

2.4.1. Cellular uptake and lysosomal co-localization of BAPCs—HeLa cells were seeded on Confocal 35 mm clear petri-dishes at a density of 1×10^4 cells/mL and grown to ~80% confluence and washed twice with PBS. Thereafter, 750 μL of fresh media was added along with a 250 μL aqueous suspension of BAPCs incorporating 30% Rhodamine B label on the bis(FLIVI)-K-K4 peptide. The final concentration of BAPCs was 50 μM. The cells were incubated for 4 h at 37 °C at 5% CO_2. After a PBS wash, the cells were then incubated for 5 min with LysoTracker® Green DND-26 probe (Molecular Probes, Carlsbad, CA) at a final concentration of 75 nM and washed again with PBS. Cells were observed and images acquired using a Zeiss LSM 510 Meta Confocal Microscope (Carl Zeiss, Gottingen, Germany).

2.4.2. Cellular uptake of BAPCs at different temperatures—HeLa cells were seeded on 12 mm culture dishes at a density of 1×10^4 cells/mL and grown to ~60% confluence. Fresh media at 4 °C and 37 °C respectively were added to the cells. Immediately thereafter, 100 μL of media was replaced by a solution of BAPCs prepared with 30% Rhodamine B label on the bis(FLIVI)-K-K_4 peptide. The final peptide concentration was 100 μM and cells were incubated for 2 h at 4 °C and 37 °C respectively. Cells were fixed with 3.7% formaldehyde at RT for 2 h, followed by a wash in PBS-T (PBS solution containing 1% Triton X-100) (Fisher Scientific LLC, Pittsburgh, PA). Subsequently, cells were incubated with Mouse Anti-β-tubulin mAb antibody [48]. 2G7D4 (Gen Script USA Inc., Piscataway, NJ) at dilutions of 1:1000 for 6 h. After three washes with PBS-T, the tissues were incubated 3 h with secondary antibody, Alexa Fluor® 488 goat anti-mouse IgG (Molecular Probes, Carlsbad, CA). Stained tissues were washed again with PBS-T and mounted in glycerol containing the nuclear stain DAPI (2 μg mL^{-1}; Sigma-Aldrich Corp., St. Louis, MO). Cells were observed and images acquired using a Zeiss LSM 510 Meta Confocal Microscope (Carl Zeiss, Gottingen, Germany).

2.5. Fluorescence and confocal microscopy

Images for Fig. 2 were taken using a LSM 700 laser scanning confocal microscope (Carl Zeiss, Gottingen, Germany) and for Fig. 3 were taken using a Zeiss LSM 510 Meta Confocal Microscope (Carl Zeiss, Gottingen, Germany). The cell boundary and structure were visualized using “differential interference contrast (DIC) microscopy”. All measurements, except where stated, were performed with un-fixed, live cells.

2.6. Protein uptake studies

HeLa cells were seeded into 11 mm wells (48-well plate) at a density of 1×10^4 cells/well and grown to roughly 60% confluence. Immediately thereafter, fresh media were added to the cells and 100 μL of the same was replaced by a solution of BAPCs containing Tcytc (5(6)-TAMRA labeled cytochrome c) and TRNase A (5(6)-TAMRA labeled RNase A) respectively. A parallel experiment was performed following the same protocol, but with Pep-1 + Tcytc and Pep-1 + TRNase A respectively, as positive controls for protein uptake. The final concentrations of peptides in each well were 50 μM for BAPCs and 5 μM for Pep-1. Cells were incubated for 3 h, washed twice with pre-warmed PBS prior to taking

epifluorescence images. Subsequently, cells were trypsinized and allowed to re-attach for 18 h and images re-acquired.

2.7. Long term cellular uptake study

HeLa cells were seeded on 11 mm culture dishes at a density of 1×10^4 cells/well and grown to ~60% confluence. Immediately thereafter, 100 μL of media was replaced by a solution of BAPCs containing 30% Rhodamine B adducted bis(FLIVI)-K-K_4; with a final BAPC concentration of 100 μM. The cells were incubated at 37 °C in an atmosphere of 5% CO_2 in air. The culture was kept for 14 days after which confocal microscopy images were acquired as previously detailed. Cells were trypsinized twice during this period and the media were replaced every 72 h.

2.8. Encapsulation and retention of ^{225}Ac in BAPCs

The bis (FLIVIGSII)-K-K_4 and bis (FLIVI)-K-K_4 peptides (100 μM ea.) were mixed in their monomeric conformation in 50% TFE/H_2O to ensure proper mixing and then dried. The dried peptides were rehydrated using a 0.15 M ammonium acetate buffer containing 100 μCi ^{225}Ac with ligand DOTA (tetraazacyclododecane-1,4,7,10-tetraacetic acid; Macrocyclics, Dallas, TX) and allowed to incubate for 2 h. Non-encapsulated radionuclide was removed by spin filtering the mixture with a 30-kDa cut-off membrane filter followed by several buffer washes. At the indicated time points, aliquots of BAPCs were withdrawn, separated from supernatant on the 30-kDa cut-off membrane filter, and the ^{225}Ac activity remaining in the BAPCs was quantified immediately and afterwards at 4 h to account for the daughters' decay on a 1282 Compugamma CS, Universal Gamma Counter (LKB Wallac, Gaithersburg, MD) equipped with the multi-channel analyzer using 150–600 keV energy window for ^{225}Ac and its daughters.

2.9. Cellular uptake of the BAPC-encapsulated ^{225}Ac into CasKi cells

CasKi cells (human metastatic cervical cancer cell line) were obtained from ATCC and grown as previously described [49]. BAPCs carrying ^{225}Ac were then used immediately to treat cells, to ensure that the BAPC diameters remain within the 50–200 nm range. Samples of 10^6 cells in triplicate were mixed with BAPC encapsulated ^{225}Ac; the cells were spun into pellet at 0, 1, 2, 4, 6 and 24 h, and the ^{225}Ac in the cellular pellet was quantified in the gamma counter as described in Section 2.8.

2.10. Biodistribution of ^{225}Ac and its daughter ^{213}Bi

All animal experiments were conducted with the permission of the Albert Einstein College of Medicine Institute for Animal Studies. ^{225}Ac was encapsulated into BAPCs by the addition of 500 μL 0.15 M ammonium acetate buffer with pH of 6.5 containing 60 μCi ^{225}Ac chloride, to 1 mM lyophilized peptides for 30 min at room temperature. After incubation the non-incorporated ^{225}Ac was removed by centrifugation on a micro-concentrator with a 30 kDa MW cut off filter. The degree of ^{225}Ac incorporation into the BAPCs was calculated to be approximately 30% of the starting amount of 60 μCi.
The ^{225}Ac-BAPCs were then diluted with sterile 0.15 M ammonium acetate buffer and eight CD-1 male mice were injected intraperitoneally (IP) with 2 μCi ^{225}Ac-BAPCs/100 μL. As

controls eight CD-1 male mice were IP injected with 2 μCi free $^{225}AcCl_3$/100 μL. At 1 and 24 h post-injection, four mice from each group were humanely sacrificed and their blood, liver, kidneys and bone were removed, weighed and counted for radioactivity in a gamma counter as described previously in Section 2.8.

3. Results and discussion

3.1. Cellular uptake of branched amphiphilic peptide capsules

In our earlier studies we noted that synthetic branched amphiphilic peptides self-assembled to form solvent filled bilayer delimited spheres (BAPCs) that had characteristic qualities (e.g., thermal, proteolytic and chaotrope stability, cellular uptake, and low cytotoxicity) that made them potential candidates for drug delivery; and as such they might provide certain advantages over conventional lipid and/or viral based drug delivery systems [38]. Apart from carrying out a number of biophysical studies we also carried out studies that characterized the initial assembly and subsequent fusion of the BAPCs. The ability to re-size and then maintain the BAPCs at fixed sizes allowed for the generation of stable capsules that could exploit cellular fenestration and transport processes [39]. These results prompted our current studies on the cellular uptake and release capabilities of these nano-capsules. We hypothesized that cellular degradative processes would eventually cause release of the encapsulated solutes within the BAPCs. Realizing that BAPCs initially form as 20–30 nm (diameter) capsules, we also wanted to determine the maximum size of a solute that could be entrapped, as well as determine the limits of percent solute encapsulation from solution during the formation of the BAPCs. Initial studies demonstrated the loading, solute retention and cellular uptake capabilities of the BAPCs by observing the in vitro cellular co-localization of two-color fluorescence from Rhodamine B labeled BAPCs incorporating 5(6)-Carboxyfluorescein solution encapsulate.

To examine cellular uptake and intra-cellular localization of BAPCs (Fig. 3); 50 μM BAPCs prepared with a 30% Rhodamine B labeled bis(FLIVI)-K-K_4 were incubated with HeLa cells for 4 h; with the lysosomes stained using LysoTracker Green DND-26, as described in Section 2.4.1. As can be seen, the stained lysosomes (green) as well as the Rhodamine B labeled BAPCs (red) are visualized in the HeLa cells, in Fig. 3A and B respectively. Upon merging the two images (Fig. 3D) both co-localized and non-co-localized BAPCs are observed, with non-co-localized particles predominating. At 2 h incubation most the BAPCs seem to be co-localized with the lysosomes (data not shown). These results indicate that BAPCs enter cells through the endosomal route yet rapidly escape the late endosomes; most likely due to lysis caused by the proposed *proton-sponge effect*, commonly observed for cationic particles [50].

In another experiment (Fig. 4) HeLa cells were treated with the Rhodamine labeled BAPCs followed by immune-fluorescence labeling prior to fixation; to monitor uptake at two different temperatures, 4 °C and 37 °C. The cell nuclei were stained with DAPI (blue) and cellular β-Tubulin was stained with Alexa Fluor® 488 goat anti-mouse IgG (green) as previously described in Section 2.4.2 Cells incubated at 37 °C (Fig. 4B) readily took up the BAPCs while those incubated at 4 °C did not; instead the BAPCs appeared to accumulate at the cell surface (Fig. 4A), presumably outside the cell.

These results indicate that cellular uptake is energy dependent. Endocytosis is a general mechanism of cellular uptake that is associated with receptor binding and/or attachment to the cellular membrane prior to internalization [51]. Non-endocytotic membrane fusion based uptake is known to be a function of the phase transition of the cellular lipid bilayer [52], whereas penetration through the cellular membrane –observed with certain polycationic cell penetrating peptides – appears to proceed in an energy independent manner [53,54]. The exact mechanism of BAPC uptake is not fully understood and might proceed via any of the above-mentioned mechanisms; however it seems conceivable based on lysosomal co-localization and temperature dependent uptake data, that BAPCs are internalized by the cellular machinery via an energy dependent endocytotic pathway. The mechanistic studies of BAPC uptake were however not the main thrust of this work.

3.2. Encapsulation and retention

Early in our work with BAPCs, we tried to encapsulate several small proteins, namely TAMRA-labeled RNase A (TRNase A, 13.7 kDa), and TAMRA-labeled cytochrome c (Tcytc, ~12 kDa), as well as the intrinsically fluorescent EGFP (26.9 kDa). These experiments were designed to test whether the BAPCs could deliver and then release the TAMRA-labeled proteins to induce a measurable cytotoxic effect. Both cytochrome c and RNase A were successfully encapsulated in the BAPCs while the EGFP which has a tendency to aggregate in water was not. In Sukthankar et al., S/TEM studies with BAPCs adducted with methyl-mercury showed that nascent BAPCs are formed with an average diameter of 20–22 nm and a calculated internal volume of 4000 nm^3 [39]. BAPCs individually loaded with Tcytc or TRNase A were incubated with HeLa cells for 3 h. Pep-1, an amphipathic cell penetrating peptide carrier capable of inducing cellular uptake of a variety of proteins and peptides into cell lines with a high degree of efficiency [55], was employed as a control delivery agent for Tcytc [56] and TRNase A.

Fig. 5 demonstrates the ability of the BAPCs to encapsulate and deliver both Tcytc and TRNase A into HeLa cells. In these representative images, the efficiency of Tcytc transport with BAPCs (Fig. 5A) is slightly less than that with Pep-1 (Fig. 5B); however in the case of TRNase A there is no significant difference between the carrying capacity of the BAPCs (Fig. 5C) versus Pep-1 (Fig. 5D). Cytochrome c [57] and RNase A [58] are both known to effect cellular apoptosis. Interestingly enough, no significant cellular apoptosis was observed in the case of either of the proteins taken up by HeLa cells using BAPCs; while Pep-1 mediated transport led to frank cytotoxicity in the expected manner (data not shown).

The ability of the BAPCs to persist within HeLa cells was then examined over a longer time period. A confocal microscopy based study conducted using HeLa cells treated with Rhodamine B labeled BAPCs (Fig. 6) revealed that even after 14 days, the BAPCs persist within the cells and are transferred to daughter cells during mitosis without any apparent degradation. The degradation of the BAPCs labeled with Rhodamine B would tend to proceed with a dispersion of the dye/dye–peptide fragments and/or an increase in the fluorescence intensity of Rhodamine B due to a change in its local environment [59]. None of these characteristics indicative of nanoparticles degrading within the cell were observed. This would – in retrospect – be consistent with expectation as cationic nano-particles,

especially those containing poly-lysine tend to escape and/or evade lysosomal degradation by charge destabilizing the endo-lysosomal membranes [60]. It seems that the cellular machinery is unable to breakdown the BAPCs. In designing the BAPCs, we anticipated that they would be able to release cargo within the cytoplasm or a cellular compartment. However, the inability of the peptide capsules to do so makes our constructs, in their current design, too stable for conventional targeted drug delivery. The peptides that constitute the BAPCs were designed to mimic diacyl phospholipids in molecular architecture. However, unlike liposomes where the non-solvated tail groups are held together primarily by hydrophobic interactions, BAPCs have the additional component of hydrogen bonding; as well as inter- and intra-molecular pi-stacking (π–π) between the phenylalanine aromatic rings of peptide sequences that apparently imbues the capsules with remarkable stability.

3.3. Encapsulation of radionuclides using BAPCs

Given the ability of BAPCs to take up but not release cargo, and their persistence in cells for extended periods of time suggested a potential application — α-particle therapy. Targeted α-particle therapy, using particle-emitting radionuclides holds promise as therapeutic agents in treating micrometastases [61]. The effectiveness of this therapy is a function of the α-particle's properties. They are emitted with energies in the MeV range, with Linear Energy Transfer (LET) having a mean energy deposition of 100 keV/μm, enabling them to produce more lethal DNA breaks per radiation track as compared to β^--particles in the cell nucleus. It has been estimated that a few α-particle transversals are sufficient to kill a cell [62]. The limited range of α-particles (50–100 μm) confines their toxicity to a small radius from the site of the isotope decay, enabling more specific tumor killing capability without damage to the surrounding normal tissue; as opposed to β^--particles, which have a much longer range [26]. Furthermore the cytocidal effectiveness of α-particles has been shown to be independent of oxygen concentration [63], dose rate and cell cycle position [64]. Additionally, studies performed on a leukemia model indicated that α-emitter radionuclides exhibited cytotoxicity superior to that of β^--radiation or γ-radiation and are capable of killing cancer cells which are resistant to chemotherapeutic drugs such as doxorubicin [65].

3.4. Targeted alpha particle therapy

There are a number of α-emitter radionuclides, one of which, ^{213}Bi ($t_{1/2}$ = 46 min), has been proposed for therapeutic use and clinically evaluated. However, ^{213}Bi is generator produced and has a relatively short half-life requiring very rapid tumor targeting. An alternative then involves utilizing ^{225}Ac, which is the parent nuclide of ^{213}Bi. A single ^{225}Ac ($t_{1/2}$ = 9.9 days) generates four alpha and three beta particles during its disintegration, along with two useful gamma emissions, including the 221 keV of ^{221}Fr and the 440 keV of ^{213}Bi (Fig. 7), that can be used for in vivo imaging [66,67]. The enhanced potency of ^{225}Ac as opposed to ^{213}Bi has been demonstrated in several pre-clinical studies [65,68]. Ongoing research has focused on harnessing the cell-killing power of these radionuclides by directing them to metastatic cells via appropriate targeting vectors.

^{225}Ac decay proceeds via a succession of daughter isotopes. This decay releases 28 MeV of energy in the form of α-particles. However, for the sake of optimal killing efficiency, the α-emissions and therefore the ^{225}Ac atom, must be delivered precisely and only to the region

of interest. A problem closely associated with the 'targeting nanogenerator approach' [69] which involves stably chelating the ^{225}Ac for delivery in vivo is that, after the initial ^{225}Ac decay to ^{221}Fr, the co-ordinate bonds from the chelating ligand to the central metal atom are not retained. Thus the daughter isotopes distribute freely within the body causing unwanted cytotoxicity.

Therefore it is desirable to confine the daughter isotopes of ^{225}Ac within the carrier during circulation and targeting. This problem is compounded by the fact that the high kinetic energy of the α-particle emissions penetrates the phospholipid membrane in liposomes, which could otherwise be considered as suitable candidates for encapsulated delivery. Moreover, the recoil trajectory of the daughter nuclides (80–90 nm) penetrates the phospholipid membranes causing rupture and leakage [31] leading to escape and redistribution within the body, increasing toxicity. Retention of daughter isotopes is size dependent. Theoretical calculations by Sofou et al. [33] suggest negligible (<0.001%) daughter retention for the last isotope for 100 nm diameter liposomes and 50% retention of the same for liposomes with a diameter larger than 650 nm. Even for giant liposomes (1 μm diameter), retention does not exceed 65%. The measured last daughter retention for the 650 nm liposomes was found to be substantially lower (11%) than what was calculated, owing to the tendency of ^{225}Ac to bind to the negatively charged phospholipid membrane leading to non-uniform distribution within the liposome causing daughter loss after recoil. The large size of such liposomes required to carry effective loads has serious limitations with regard to fenestration and cellular uptake. This coupled with low daughter retention capabilities makes them a cumbersome system for efficient targeted radiotherapy. Considering the stability, uptake and retentive capabilities of the BAPCs; they were tested as a potential ^{225}Ac carrier for targeted alpha particle therapy applications.

3.5. Radio-therapeutic potential of BAPCs

Experiments were performed to monitor encapsulation of ^{225}Ac into BAPCs, as well as its retention within them over 7 days. Uptake of BAPC-encapsulated ^{225}Ac was then tested in vitro using human metastatic cervical cancer (CasKi) cells. The ^{225}Ac was well contained by the BAPCs, with retention being ≥95% of the original activity for the period of 7 days (Fig. 8A). The cellular uptake of encapsulated ^{225}Ac increased in a time dependent manner and reached 33% at 24 h post incubation (Fig. 8B). It is important to note that a much lower dose of ^{225}Ac (0.1 μCi) was used for this uptake experiment to avoid any cytocidal effects on the cells that could cloud the cellular uptake results. These findings were encouraging as they demonstrated the potential of BAPCs as candidates for ^{225}Ac encapsulation and cellular uptake.

3.6. Biodistribution of BAPCs encapsulating ^{225}Ac

To investigate the behavior of BAPCs in vivo we studied the distribution of BAPC encapsulated ^{225}Ac and its daughter ^{213}Bi (along with a control of free $^{225}AcCl_3$ and ^{213}Bi), in CD1 mice at 1 and 24 h post IP administration. Tissues were collected and analyzed at the indicated times. The 440 keV γ-emission of ^{213}Bi was used to calculate the percentage of the injected dose per gram of organ (ID/g organ, %) as described in Section 2.10. In Fig. 9 we see the results of the in vivo distribution in mice for free ^{213}Bi/^{225}Ac versus encapsulated

material. At 1 h post injection, when both 'BAPC encapsulated ^{225}Ac' and 'free ^{225}Ac' were still in the process of exiting the peritoneal cavity, there was no significant difference in organ uptake between BAPC encapsulated ^{225}Ac and free ^{225}Ac (except for bone, where free ^{225}Ac is known to accumulate). The uptake of ^{225}Ac daughter ^{213}Bi into the kidneys was higher than that of ^{225}Ac, as free ^{213}Bi targets kidneys. The differences between BAPC encapsulated ^{225}Ac, and free ^{225}Ac became more pronounced at 24 h post injection. The free ^{225}Ac is completely cleared from the blood via binding to the plasma proteins and being delivered to various organs. BAPC encapsulated ^{225}Ac stayed in circulation due to the small size of the BAPCs, consistent with nanomaterials in the 10–20 nm size range that tend to stay in circulation. Free ^{225}Ac accumulated significantly more in the liver ($P = 0.03$) and in the bone ($P = 0.02$) than the BAPC encapsulated ^{225}Ac. This confirms the tight retention of ^{225}Ac within the vesicles. ^{213}Bi daughter was present together with ^{225}Ac pointing to retention of the daughters by the BAPCs as well. The only organ where there was more ^{213}Bi present in comparison with ^{225}Ac were the kidneys — which serve as the 'sink' for ^{213}Bi that has been released from any organ in the body. Overall, encapsulated ^{225}Ac cleared much more from the body than 'free ^{225}Ac' through the combination of renal, hepatobiliary and intestinal goblet cell (GC) secretion (IGCSP) pathways [70]. Taken together, these results point to the ability of BAPCs to incorporate and retain ^{225}Ac and its daughter isotopes through ^{213}Bi.

4. Conclusion

It is evident that the extraordinary stability of the BAPCs, in their current design, limits their use as a drug delivery modality. However, this same characteristic makes them appear ideal for targeted alpha particle therapy for the treatment of metastatic and infectious diseases. Our results show that alpha the emitting radionuclide ^{225}Ac, and its radioactive daughters, can be sequestered within the lumen of the BAPCs and then retained for days (and through multiple cell divisions), just outside the nucleus of the cell. This portends well for cytocidal effects.

The fact that BAPCs withstand rupture from the ejected high energy alpha particles and the resulting recoil of the daughter isotope, suggests a self-annealing property for BAPCs. It is likely that BAPCs are taken up by cells through a non-selective internalization process, possibly proceeding via transient pore formation, analogous to that observed with some polycationic lipids [71] and polymers [72]. Should this assessment be accurate; the BAPCs would be able to find utility as nano-carriers in cellular systems. The poly-lysine cationic surface of the BAPCs provides a convenient synthetic pathway for the modification and conjugation of ligands, antibodies and molecular markers to achieve cellular targeting. This could greatly reduce the whole body load required to kill desired cells as well as reduce deleterious off-target side effects. The fact that the capsules also remain in circulation for an extended period most likely reflects their small size and flexibility. The ability of the BAPCs to persist in cells through cell division(s) suggests a potential use as cell lineage tracers and probes. BAPCs could be conjugated to quantum dots in an effort to resolve some of the biocompatibility issues associated with the latter [73]. The BAPCs constitute a unique and exciting new class of biomaterial, which while portending promise as a convenient agent for targeted alpha particle therapy, could find application in many other areas as well.

Acknowledgments

Funding sources

Partial support for this project was provided by PHS-NIH grants GM 074096 (to J.M.T.) and GM021784 (to R.P.H.) and the Terry Johnson Cancer Center for summer support (to P.S.)

This is publication 14-166-J from the Kansas Agricultural Experiment Station. We would like to thank Dr. Stella Y Lee, Division of Biology, Kansas State University, for providing us with HeLa cell lines and, Dr. David Moore and Heather Shinogle at the University of Kansas Microscopy and Analytical Imaging Laboratory, for long term cellular uptake studies.

Abbreviations

BAPCs	branched amphiphilic peptide capsules
DMEM	Dulbecco's minimum essential medium
FBS	fetal bovine serum
TFE	2,2,2-Trifluoroethanol
DAPI	2-(4-amidinophenyl)-1H-indole-6-carboxamidine
CD	circular dichroism spectroscopy
DLS	dynamic light scattering or photon correlation spectroscopy
S/TEM	scanning transmission electron microscopy
EM	electron microscopy
Tcytc	5(6)-TAMRA labeled cytochrome c
TRNase A	5(6)-TAMRA labeled RNase A
EDTA	2-({2-[bis(carboxymethyl)amino]ethyl}(carboxymethyl) amino)acetic acid
DTPA	Penta(carboxymethyl)diethylenetriamine
DOTA	2-[4-nitrobenzyl]-1, 4, 7, 10-tetraazacyclododecane-N,N′,N″, N‴-tetraacetic acid
HEHA	1,4,7,10,13,16-hexaazacyclohexadecane-N,N′,N″,N‴,N⁗,N⁗′ - hexa-acetic acid
PEPA	2-[4-nitrobenzyl]-1,4,7,10,13-pentaazacyclopentadecane-N, N′,N″,N‴,N⁗-pentaacetic acid
TETA	2-[4-nitrobenzyl]-1, 4, 8, 11-tetraazacyclotetradecane N,N′,N ″,N‴-tetraacetic acid

References

1. Douglas SJ, Davis SS, Illum L. Nanoparticles in drug delivery. Crit Rev Ther Drug Carrier Syst. 1987; 3:233–261. [PubMed: 3549008]
2. Gref R, Domb A, Quellec P, Blunk T, Müller RH, Verbavatz JM, Langer R. The controlled intravenous delivery of drugs using PEG-coated sterically stabilized nanospheres. Adv Drug Deliv Rev. 1995; 16:215–233.

3. Harashima H, Sakata K, Funato K, Kiwada H. Enhanced hepatic uptake of liposomes through complement activation depending on the size of liposomes. Pharm Res. 1994; 11:402–406. [PubMed: 8008707]
4. Devine DV, Wong K, Serrano K, Chonn A, Cullis PR. Liposome-complement interactions in rat serum: implications for liposome survival studies. Biochim Biophys Acta. 1994; 1191:43–51. [PubMed: 8155683]
5. Dunn SE, Brindley A, Davis SS, Davies MC, Illum L. Polystyrene–poly (ethylene glycol) (PS-PEG2000) particles as model systems for site specific drug delivery. 2. The effect of PEG surface density on the in vitro cell interaction and in vivo biodistribution. Pharm Res. 1994; 11:1016–1022. [PubMed: 7937542]
6. Gref R, Minamitake Y, Peracchia M, Trubetskoy V, Torchilin V, Langer R. Biodegradable long-circulating polymeric nanospheres. Science. 1994; 263:1600–1603. [PubMed: 8128245]
7. Alexis F, Pridgen E, Molnar LK, Farokhzad OC. Factors affecting the clearance and biodistribution of polymeric nanoparticles. Mol Pharm. 2008; 5:505–515. [PubMed: 18672949]
8. Kim SY, Shin IG, Lee YM, Cho CS, Sung YK. Methoxy poly(ethylene glycol) and epsilon–caprolactone amphiphilic block copolymeric micelle containing indometh-acin. II. Micelle formation and drug release behaviours. J Control Release. 1998; 51:13–22. [PubMed: 9685900]
9. Kim SY, Shin IG, Lee YM. Amphiphilic diblock copolymeric nanospheres composed of methoxy poly(ethylene glycol) and glycolide: properties, cytotoxicity and drug release behaviour. Biomaterials. 1999; 20:1033–1042. [PubMed: 10378803]
10. Liu J, Xiao Y, Allen C. Polymer–drug compatibility: a guide to the development of delivery systems for the anticancer agent, ellipticine. J Pharm Sci. 2004; 93:132–143. [PubMed: 14648643]
11. Letchford K, Burt H. A review of the formation and classification of amphiphilic block copolymer nanoparticulate structures: micelles, nanospheres, nanocapsules and polymersomes. Eur J Pharm Biopharm. 2007; 65:259–269. [PubMed: 17196803]
12. Discher DE, Ahmed F. Polymersomes. Annu Rev Biomed Eng. 2006; 8:323–341. [PubMed: 16834559]
13. Soppimath KS, Aminabhavi TM, Kulkarni AR, Rudzinski WE. Biodegradable polymeric nanoparticles as drug delivery devices. J Control Release. 2001; 70:1–20. [PubMed: 11166403]
14. Mora-Huertas CE, Fessi H, Elaissari A. Polymer-based nanocapsules for drug delivery. Int J Pharm. 2010; 385:113–142. [PubMed: 19825408]
15. Besnard R, Cambedouzou J, Arrachart G, Diat O, Pellet-Rostaing S. Self-assembly of condensable bola-amphiphiles in water/tetraethoxysilane mixtures for the elaboration of mesostructured hybrid materials. Langmuir. 2013; 29:10368–10375. [PubMed: 23879565]
16. Yan Y, Lu T, Huang J. Recent advances in the mixed systems of bolaamphiphiles and oppositely charged conventional surfactants. J Colloid Interface Sci. 2009; 337:1–10. [PubMed: 19486992]
17. Bianco A, Kostarelos K, Prato M. Applications of carbon nanotubes in drug delivery. Curr Opin Chem Biol. 2005; 9:674–679. [PubMed: 16233988]
18. Kazi KM, Mandal AS, Biswas N, Guha A, Chatterjee S, Behera M, Kuotsu K. Niosome: a future of targeted drug delivery systems. J Adv Pharm Technol Res. 2010; 1:374–380. [PubMed: 22247876]
19. Yasam, VR.; Jakki, SL.; Natarajan, J.; Kuppusamy, G. A review on novel vesicular drug delivery: proniosomes. Drug Deliv. 2013. http://dx.doi.org/10.3109/10717544.2013 (Epub ahead of print)
20. Hu C, Rhodes DG. Proniosomes: a novel drug carrier preparation. Int J Pharm. 1999; 185:23–35. [PubMed: 10425362]
21. Hillaireau H, Couvreur P. Nanocarriers' entry into the cell: relevance to drug delivery. Cell Mol Life Sci. 2009; 66:2873–2896. [PubMed: 19499185]
22. Imam SK. Advancements in cancer therapy with alpha-emitters: a review. Int J Radiat Oncol Biol Phys. 2001; 51:271–278. [PubMed: 11516878]
23. Davis IA, Glowienka KA, Boll RA, Deal KA, Brechbiel MW, Stabin M, Bochsler PN, Mirzadeh S, Kennel SJ. Comparison of ^{225}actinium chelates: tissue distribution and radiotoxicity. Nucl Med Biol. 1999; 26:581–589. [PubMed: 10473198]
24. Schwartz J, Jaggi JS, O'Donoghue JA, Ruan S, McDevitt M, Larson SM, Scheinberg DA, Humm JL. Renal uptake of ^{213}bismuth and its contribution to kidney radiation dose following

administration of ^{225}actinium-labeled antibody. Phys Med Biol. 2011; 56:721–733. [PubMed: 21220845]

25. Jaggi JS, Seshan SV, McDevitt MR, LaPerle K, Sgouros G, Scheinberg DA. Renal tubulointerstitial changes after internal irradiation with alpha-particle-emitting actinium daughters. J Am Soc Nephrol. 2005; 16:2677–2689. [PubMed: 15987754]
26. Kim YS, Brechbiel MW. An overview of targeted alpha therapy. Tumour Biol. 2012; 33:573–590. [PubMed: 22143940]
27. Deal KA, Davis IA, Mirzadeh S, Kennel SJ, Brechbiel MW. Improved in vivo stability of actinium-225 macrocyclic complexes. J Med Chem. 1999; 42:2988–2992. [PubMed: 10425108]
28. Hider RC, Hall AD. Clinically useful chelators of tripositive elements. Prog Med Chem. 1991; 28:41–173. [PubMed: 1843549]
29. Chappell LL, Deal KA, Dadachova E, Brechbiel MW. Synthesis, conjugation, and radiolabeling of a novel bifunctional chelating agent for ^{225}Ac radioimmunotherapy applications. Bioconjug Chem. 2000; 11:510–519. [PubMed: 10898572]
30. Henriksen G, Schoultz BW, Michaelsen TE, Bruland ØS, Larsen RH. Sterically stabilized liposomes as a carrier for α-emitting radium and actinium radionuclides. Nucl Med Biol. 2004; 31:441–449. [PubMed: 15093814]
31. Sofou S, Thomas JL, Lin HY, McDevitt MR, Scheinberg DA, Sgouros G. Engineered liposomes for potential alpha-particle therapy of metastatic cancer. J Nucl Med. 2004; 45:253–260. [PubMed: 14960644]
32. Sofou S, Kappel BJ, Jaggi JS, McDevitt MR, Scheinberg DA, Sgouros G. Enhanced retention of the alpha-particle-emitting daughters of ^{225}Actinium by liposome carriers. Bioconjug Chem. 2007; 18:2061–2067. [PubMed: 17935286]
33. McDevitt MR, Finn RD, Sgouros G, Ma D, Scheinberg DA. An ^{225}Ac/^{213}Bi generator system for therapeutic clinical applications: construction and operation. Appl Radiat Isot. 1999; 50:895–904. [PubMed: 10214708]
34. Nikula TK, McDevitt MR, Finn RD, Wu C, Kozak RW, Garmestani K, Brechbiel MW, Curcio MJ, Pippin CG, Tiffany-Jones L, Geerlings MW Sr, Apostolidis C, Molinet R, Geerlings MW Jr, Gansow OA, Scheinberg DA. Alpha-emitting bismuth cyclohexylbenzyl DTPA constructs of recombinant humanized anti-CD33 antibodies: pharmacokinetics, bioactivity, toxicity and chemistry. J Nucl Med. 1999; 40:166–176. [PubMed: 9935073]
35. Chakrabarti MC, Le N, Paik CH, De Graff WG, Carrasquillo JA. Prevention of radi-olysis of monoclonal antibody during labeling. J Nucl Med. 1996; 37:1384–1388. [PubMed: 8708780]
36. Stensrud G, Redford K, Smistad G, Karlsen J. Effects of gamma irradiation on solid and lyophilised phospholipids. Radiat Phys Chem. 1999; 56:611–622.
37. Couvreur P. Nanoparticles in drug delivery: past, present and future. Adv Drug Deliv Rev. 2013; 65:21–23. [PubMed: 22580334]
38. Gudlur S, Sukthankar P, Gao J, Avila LA, Hiromasa Y, Chen J, Iwamoto T, Tomich JM. Peptide nanovesicles formed by the self-assembly of branched amphiphilic peptides. PLoS One. 2012; 7:e45374. [PubMed: 23028970]
39. Sukthankar, P.; Gudlur, S.; Avila Flores, LA.; Whitaker, SK.; Katz, BB.; Hiromasa, Y.; Gao, J.; Thapa, PS.; Moore, DS.; Iwamoto, T.; Chen, J.; Tomich, JM. Branched oligopeptides form nano-capsules with lipid vesicle characteristics. Langmuir. Nov 18. 2013 http://dx.doi.org/10.1021/la403492n (Epub ahead of print)
40. Grove A, Tomich JM, Iwamoto T, Montal M. Design of a functional calcium channel protein: inferences about an ion channel-forming motif derived from the primary structure of voltage-gated calcium channels. Protein Sci. 1993; 2:1918–1930. [PubMed: 7505682]
41. Kempe M, Barany G. CLEAR: a novel family of highly cross-linked polymeric supports for solid phase synthesis. J Am Chem Soc. 1996; 118:7083–7093.
42. Iwamoto T, Grove A, Montal MO, Montal M, Tomich JM. Chemical synthesis and characterization of peptides and oligomeric proteins designed to form transmembrane ion channels. Int J Pept Protein Res. 1994; 43:597–607. [PubMed: 7523324]

43. Pietta PG, Cavallo PF, Takahashi K, Marshall GR. Preparation and use of benzhydrylamine polymers in peptide synthesis. II. Synthesis of thyrotropin releasing hormone, thyrocalcitonin 26–32, and eledoisin. J Org Chem. 1974; 39:44–48. [PubMed: 4206303]
44. Pennington, MW. HF Cleavage and Deprotection Procedures for Peptides Synthesized Using a Boc/Bzl Strategy in Peptide Synthesis Protocols. Pennington, MW.; Dunn, BM., editors. Vol. 35. Humana Press; 1994. p. 41-62.
45. Tomich JM, Carson LW, Kanes KJ, Vogelaar NJ, Emerling MR, Richards JH. Prevention of aggregation of synthetic membrane-spanning peptides by addition of detergent. Anal Biochem. 1988; 174:197–203. [PubMed: 3218732]
46. Chen RF. Measurements of absolute values in biochemical fluorescence spectroscopy. J Res Natl Bur Stand. 1972; 76A(6):593–606.
47. Sponer H. Remarks on the absorption spectra of phenylalanine and tyrosine in connection with the absorption in toluene and paracresol. J Chem Phys. 1942; 10:672.
48. Geisert EE Jr, Frankfurter A. The neuronal response to injury as visualized by immunostaining of class III β-tubulin in the rat. Neurosci Lett. 1989; 102:137–141. [PubMed: 2682386]
49. Harris M, Wang XG, Jiang Z, Phaeton R, Koba W, Goldberg GL, Casadevall A, Dadachova E. Combined treatment of the experimental human papilloma virus-16-positive cervical and head and neck cancers with cisplatin and radioimmunotherapy targeting viral E6 oncoprotein. Br J Cancer. 2013; 108(4):859–865. [PubMed: 23385729]
50. Midoux P, Pichon C, Yaouanc JJ, Jaffrès PA. Chemical vectors for gene delivery: a current review on polymers, peptides and lipids containing histidine or imidazole as nucleic acids carriers. Br J Pharmacol. 2009; 157(2):166–178. [PubMed: 19459843]
51. Xiang S, Tong H, Shi Q, Fernandes JC, Jin T, Dai K, Zhang X. Uptake mechanisms of non-viral gene delivery. J Control Release. 2012; 158:371–378. [PubMed: 21982904]
52. Melchior DL, Morowitz HJ, Sturtevant JM, Tsong TY. Characterization of the plasma membrane of Mycoplasma laidlawii. VII. Phase transitions of membrane lipids. Biochim Biophys Acta Biomembr. 1970; 219:114–122.
53. Madani, F.; Lindberg, S.; Langel, Ü.; Futaki, S.; Gräslund, A. Mechanisms of cellular uptake of cell-penetrating peptides. J Biophys. 2011. http://dx.doi.org/10.1155/2011/414729
54. Gupta B, Levchenko TS, Torchilin VP. Intracellular delivery of large molecules and small particles by cell-penetrating proteins and peptides. Adv Drug Deliv Rev. 2005; 57:637–651. [PubMed: 15722168]
55. Morris MC, Depollier J, Mery J, Heitz F, Divita G. A peptide carrier for the delivery of biologically active proteins into mammalian cells. Nat Biotechnol. 2001; 19:1173–1176. [PubMed: 11731788]
56. Fawell S, Seery J, Daikh Y, Moore C, Chen LL, Pepinsky B, Barsoum J. Tat-mediated delivery of heterologous proteins into cells. Proc Natl Acad Sci U S A. 1994; 91:664–668. [PubMed: 8290579]
57. Zhivotovsky B, Orrenius S, Brustugun OT, Doskeland SO. Injected cytochrome c induces apoptosis. Nature. 1998; 391:449–450. [PubMed: 9461210]
58. Kim JS, Soucek J, Matousek J, Raines RT. Mechanism of ribonuclease cytotoxicity. J Biol Chem. 1995; 270:31097–31102. [PubMed: 8537370]
59. Romero G, Echeverria M, Qiu Y, Murray RA, Moya SE. A novel approach to monitor intracellular degradation kinetics of poly(lactide-co-glycolide) nanoparticles by means of flow cytometry. J Mater Chem B. 2014; 2:826–833.
60. Panyam J, Zhou WZ, Prabha S, Sahoo SK, Labhasetwar V. Rapid endo-lysosomal escape of poly(DL-lactide-co-glycolide) nanoparticles: implications for drug and gene delivery. FASEB J. 2002; 16:1217–1226. (United States). [PubMed: 12153989]
61. Couturier O, Supiot S, Degraef-Mougin M, Faivre-Chauvet A, Carlier T, Chatal JF, Davodeau F, Cherel M. Cancer radioimmunotherapy with alpha-emitting nuclides. Eur J Nucl Med Mol Imaging. 2005; 32:601–614. [PubMed: 15841373]
62. Sgouros G, Roeske JC, McDevitt MR, Palm S, Allen BJ, Fisher DR, Brill AB, Song H, Howell RW, Akabani G, Bolch WE, Brill AB, Fisher DR, Howell RW, Meredith RF, Sgouros G, Wessels BW, Zanzonico PB. SNMMIRDCommittee. MIRD Pamphlet No. 22 (abridged): radiobiology and

dosimetry of alpha-particle emitters for targeted radionuclide therapy. J Nucl Med. 2010; 51:311–328. [PubMed: 20080889]

63. Wulbrand C, Seidl C, Gaertner FC, Bruchertseifer F, Morgenstern A, Essler M, Senekowitsch-Schmidtke R. Alpha-particle emitting ^{213}Bi-anti-EGFR immunoconjugates eradicate tumor cells independent of oxygenation. PLoS One. 2013; 8(5):e64730. [PubMed: 23724085]
64. Miederer M, Scheinberg DA, McDevitt MR. Realizing the potential of the Actinium-225 radionuclide generator in targeted alpha particle therapy applications. Adv Drug Deliv Rev. 2008; 60:1371–1382. [PubMed: 18514364]
65. Friesen C, Glatting G, Koop B, Schwarz K, Morgenstern A, Apostolidis C, Debatin KM, Reske SN. Breaking chemoresistance and radioresistance with [213Bi] anti-CD45 antibodies in leukemia cells. Cancer Res. 2007; 67:1950–1958. [PubMed: 17332322]
66. Suliman G, Pommé S, Marouli M, Van Ammel R, Stroh H, Jobbágy V, Paepen J, Dirican A, Bruchertseifer F, Apostolidis C, Morgenstern A. Half-lives of ^{221}Fr, ^{217}At, ^{213}Bi, ^{213}Po and ^{209}Pb from the ^{225}Ac decay series. Appl Radiat Isot. 2013; 77:32–37. [PubMed: 23511775]
67. Pommé S, Marouli M, Suliman G, Dikmen H, Van Ammel R, Jobbágy V, Dirican A, Stroh H, Paepen J, Bruchertseifer F, Apostolidis C, Morgenstern A. Measurement of the ^{225}Ac half-life. Appl Radiat Isot. 2012; 70(11):2608–2614. [PubMed: 22940415]
68. McDevitt MR, Barendswaard E, Ma D, Lai L, Curcio MJ, Sgouros G, Ballangrud AM, Yang WH, Finn RD, Pellegrini V, Geerlings MW Jr, Lee M, Brechbiel MW, Bander NH, Cordon-Cardo C, Scheinberg DA. An alpha-particle emitting antibody ([^{213}Bi]J591) for radioimmunotherapy of prostate cancer. Cancer Res. 2000; 60:6095–6100. [PubMed: 11085533]
69. McDevitt MR, Ma D, Lai LT, Simon J, Borchardt P, Frank RK, Wu K, Pellegrini V, Curcio MJ, Miederer M, Bander NH, Scheinberg DA. Tumor therapy with targeted atomic nanogenerators. Science. 2001; 294:1537–1540. [PubMed: 11711678]
70. Zhao B, Sun L, Zhang W, Wang Y, Zhu Z, Zhu X, Yang L, Li C, Zhang Z, Zhang Y. Secretion of intestinal goblet cells: a novel excretion pathway of nanoparticles. Nanomedicine, NBM. 2013
71. Hafez IM, Maurer N, Cullis PR. On the mechanism whereby cationic lipids promote intracellular delivery of polynucleic acids. Gene Ther. 2001; 8:1188–1196. [PubMed: 11509950]
72. Hong S, Bielinska AU, Mecke A, Keszler B, Beals JL, Shi X, Balogh L, Orr BG, Baker JR Jr, Banaszak Holl MM. Interaction of poly(amidoamine) dendrimers with supported lipid bilayers and cells: hole formation and the relation to transport. Bioconjug Chem. 2004; 15:774–782. [PubMed: 15264864]
73. Alivisatos AP, Gu W, Larabell C. Quantum dots as cellular probes. Annu Rev Biomed Eng. 2005; 7:55–76. [PubMed: 16004566]

Fig. 1.
Bilayer forming branched amphiphilic peptide sequences.

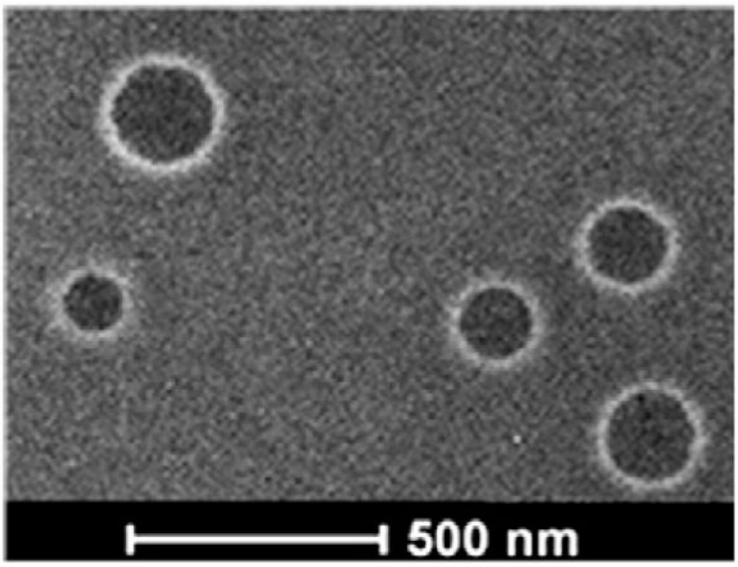

Fig. 2.

S/TEM image of BAPCs. They containing 30% Hg label and imaged at 2 h post hydration w/negative glow discharge and uranyl acetate staining prepared as previously described [39].

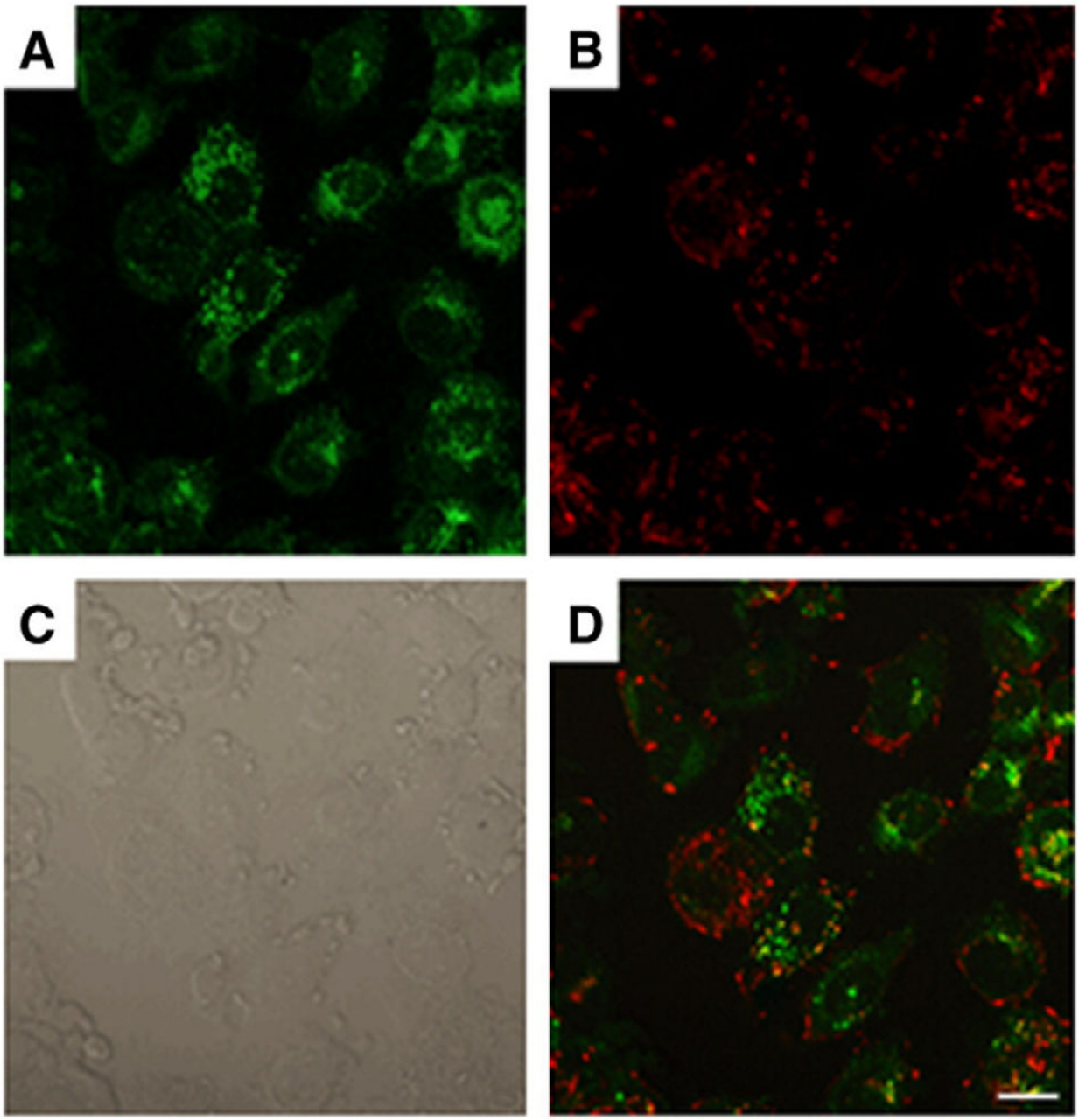

Fig. 3.

Lysosomal co-localization of BAPCs. Confocal microscopy analysis of HeLa cells incubated at 37 °C with 50 μM 30% Rhodamine B labeled BAPCs for 4 h. A) HeLa cells with lysosomal stain (green); B) Rhodamine B labeled BAPCs (red); C) bright field image; D) merge image showing co-localization of BAPCs and the lysosomes (yellow). Scale bar = 20 μm.

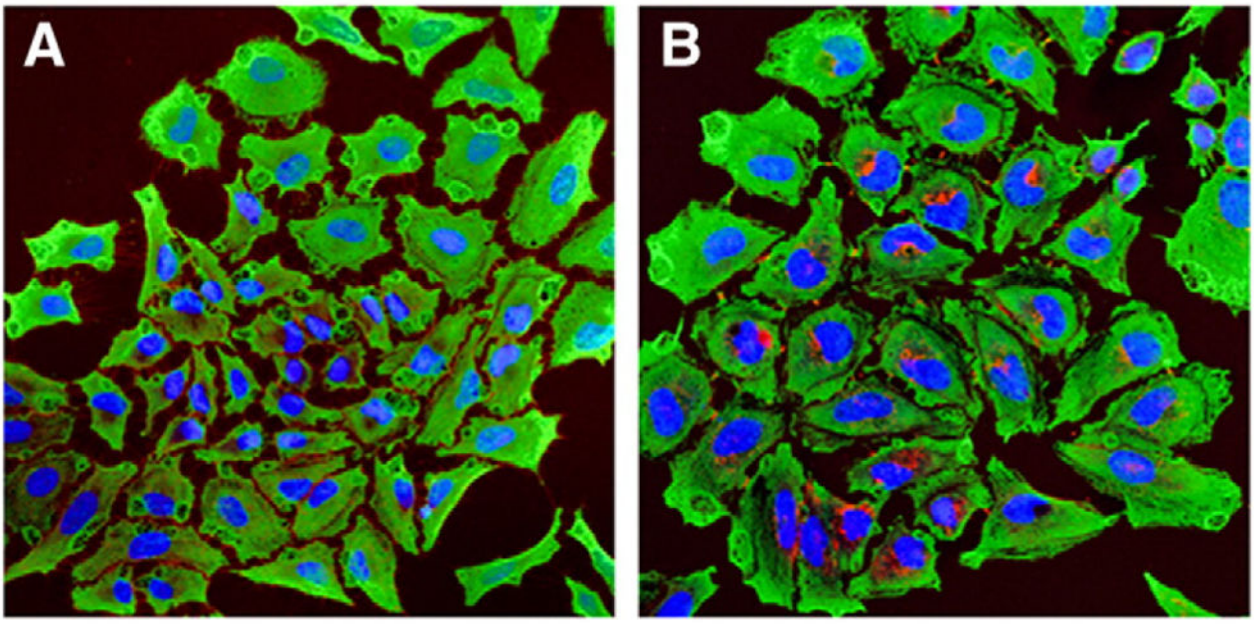

Fig. 4.

Temperature dependence of cellular uptake. Confocal microscopy analysis of HeLa cells incubated with 100 μM 30% Rhodamine B labeled BAPCs for 2 h. A) HeLa cells at 4 °C and B) at 37 °C.

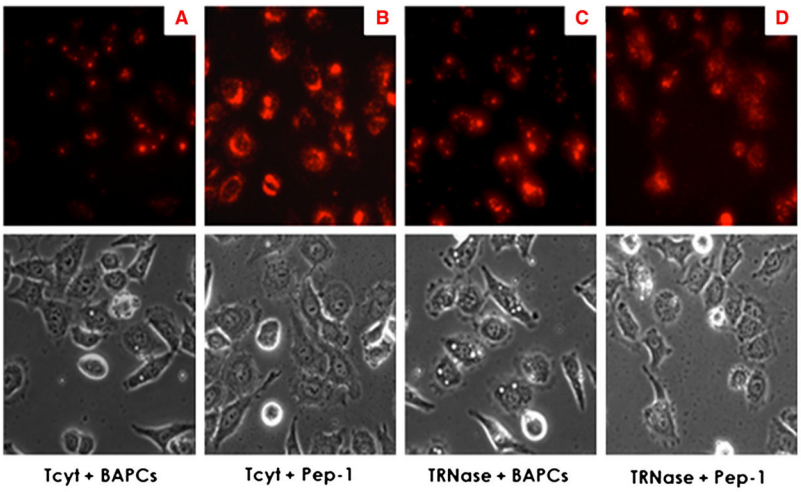

Fig. 5.

TAMRA labeled protein uptake in HeLa cells. Fluorescence microscopy images of HeLa cells after 3 h of incubation. The lower panel shows DIC images. A) BAPCs with Tcytc; B) Tcytc with Pep-1; C) BAPCs with TRNAse A; D) TRNase A with Pep-1.

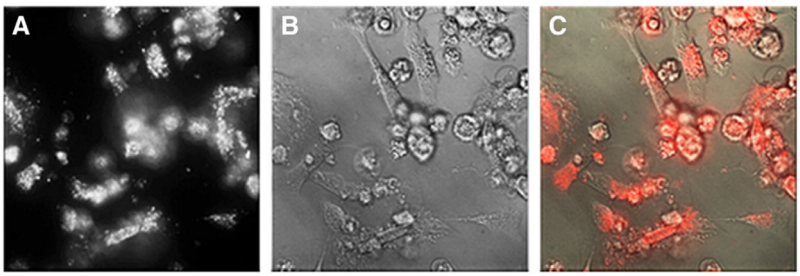

Fig. 6.

Long term cell uptake study. HeLa cells incubated with BAPCs with a 30% Rhodamine B label on bis(FLIVI)-K-K_4, observed after 2 weeks using confocal microscopy through two trypsinizations. A) Dark field image with channel selected for the excitation of Rhodamine; B) bright-field image; C) overlap of the bright-field image and channel for Rhodamine.

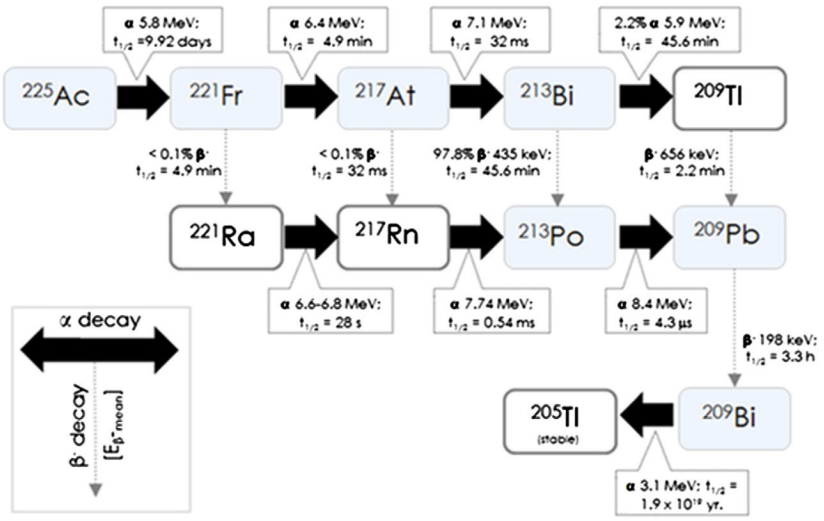

Fig. 7.

The proposed decay scheme for ^{225}Ac based on the recently published studies [64,65].

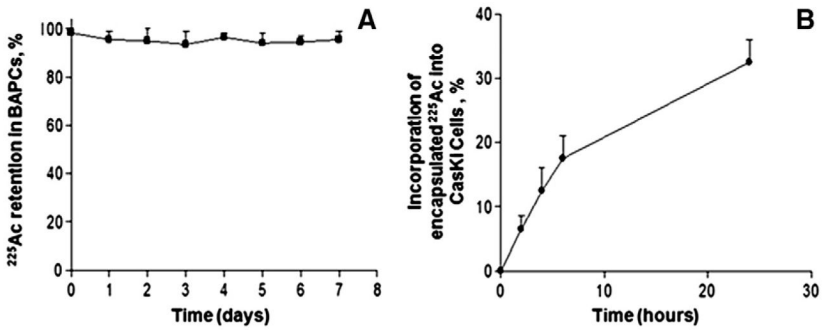

Fig. 8.

Cellular uptake and retention of BAPCs encapsulated with ^{225}Ac. A) Encapsulation and retention of ^{225}Ac within BAPCs over 7 days and B) cellular uptake of the BAPC-encapsulated ^{225}Ac into CasKi cells over 24 h.

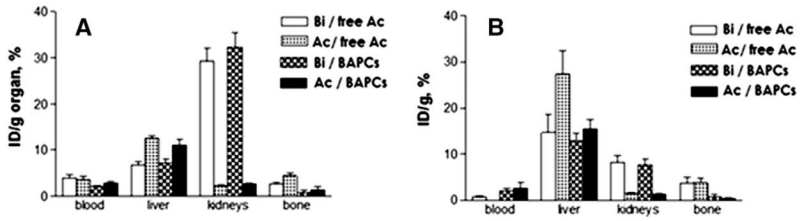

Fig. 9.

Biodistribution of free and BAPC-encapsulated, ^{225}Ac and its daughter ^{213}Bi, in CD1 mice. A) 1 h time point; B) 24 h time point.